PCCP

PAPER

View Article Online
View Journal | View Issue

Cite this: *Phys. Chem. Chem. Phys.*, 2014, **16**, 5723

Molecular interactions in aqueous biphasic systems composed of polyethylene glycol and crystalline *vs.* liquid cholinium-based salts†

Jorge F. B. Pereira,[ab] Kiki A. Kurnia,[a] O. Andreea Cojocaru,[b] Gabriela Gurau,[b] Luís Paulo N. Rebelo,[c] Robin D. Rogers,*[b] Mara G. Freire*[ac] and João A. P. Coutinho[a]

Received 20th November 2013,
Accepted 27th January 2014

DOI: 10.1039/c3cp54907k

www.rsc.org/pccp

The relative ability of cholinium-($[Ch]^+$)-based salts, including ionic liquids (ILs), to form biocompatible aqueous biphasic systems (ABS) with polyethylene glycols (PEGs) was deeply scrutinized in this work. Aqueous solutions of low molecular weight PEG polymers (400, 600, and 1000 g mol^{-1}) and $[Ch]^+$ salts of chloride, acetate, bicarbonate, glycolate, lactate, dihydrogenphosphate, dihydrogencitrate, and bitartrate can undergo liquid–liquid demixing at certain concentrations of the phase-forming components and at several temperatures. Cholinium butanoate and propanoate were also studied; however, these long alkyl side chain ILs are not able to promote an immiscibility region with PEG aqueous solutions. The ternary liquid–liquid phase diagrams, binary water activities, PEG–salt and salt–H_2O solubility data, and binary and ternary excess enthalpies estimated by COSMO-RS (COnductor-like Screening MOdel for Realistic Solvation) were used to obtain new insights into the molecular-level mechanisms responsible for phase separation. Instead of the expected and commonly reported salting-out phenomenon induced by the $[Ch]^+$ salts over the polymer, the formation of PEG–$[Ch]^+$ salt ABS was revealed to be an end result of a more intricate molecular scenario. The multifaceted approach employed here reveals that the ability to promote an ABS is quite different for the higher melting salts *vs.* the lower melting or liquid ILs. In the latter systems, the ABS formation seems to be controlled by the interplay of the relative strengths of the ion–ion, ion–water, ion–PEG, and water–PEG interactions, with a significant contribution from specific hydrogen-bonding between the IL anion and the PEG hydroxyl groups.

Introduction

Aqueous biphasic systems (ABS) are formed by the combination of two distinct species dissolved in aqueous media, *e.g.* polymer–polymer, polymer–salt or salt–salt mixtures.[1] Although both solutes are water-soluble, at least to a large extent, above given concentrations the ternary systems undergo liquid–liquid demixing. ABS are thus composed of two macroscopic aqueous-rich phases and these have emerged as sustainable and biocompatible alternatives to more conventional liquid–liquid extraction processes which often employ volatile and hazardous organic solvents.[1] In fact, in the last mid-century, ABS were proposed for use in novel and efficient techniques for the separation, purification and recovery of different biological compounds, such as proteins, enzymes, and blood cells.[1]

Traditionally, ABS are formed by combining aqueous solutions of two hydrophilic polymers, such as polyethylene glycol (PEG) and dextran, or alternatively, a polymer and an inorganic salt, such as the PEG–sodium phosphate system.[2] Recently, other species, namely proteins or surfactants, have also been studied to induce the formation of ABS when mixed with polymers or salts.[3] However, of all the solutes capable of forming ABS, the recent application of ionic liquids (ILs) appears to be one of the most attractive. In 2003, one of us showed that ABS could be formed by mixing a hydrophilic IL and a high charge density inorganic salt.[4]

ILs are commonly defined as ionic compounds with melting temperatures lower than 100 °C, and many examples exhibit negligible vapour pressure, high thermal and chemical stabilities, and improved capacity to solvate a wide array of compounds.[5]

[a] *Departamento de Química, CICECO, Universidade de Aveiro, Campus Universitário de Santiago, 3810-193 Aveiro, Portugal. E-mail: maragfreire@ua.pt; Fax: +351 234 370084; Tel: +351 234 370200*
[b] *Center for Green Manufacturing and Department of Chemistry, The University of Alabama, Tuscaloosa, AL 35487, USA. E-mail: rdrogers@ua.edu*
[c] *Instituto de Tecnologia Química e Biológica, ITQB2, Universidade Nova de Lisboa, Av. República, Apartado 127, 2780-901 Oeiras, Portugal. Web: www.itqb.unl.pt*

† Electronic supplementary information (ESI) available: Experimental weight fraction data; tie-line and tie-line length data; conductivities and pH values of the coexisting phases; additional representation of the remaining ABS; COSMO-RS prediction results. See DOI: 10.1039/c3cp54907k

In addition, the tunability of the IL physicochemical properties, resulting from an appropriate combination of their ions, allows one to prepare task-specific solvents for separation, reaction, and purification processes.

A recent review on IL-based ABS addressed their phase diagrams, their relative ability to form, and highlighted their excellent performance in the extraction of targeted biomolecules.[6] In particular, IL-based ABS have shown better extractive performance over conventional polymer-based systems, since the limited hydrophobic–hydrophilic range exhibited by the coexisting phases constituted by two polymers or one polymer and an inorganic salt is overcome when employing ILs.[7] Even when dealing with conventional ABS, the addition of small amounts of ILs as adjuvants allows the adjustment of the intrinsic properties of the coexisting phases and tuning of the extraction efficiencies for a given product.[8]

The observation of immiscibility domains in mixtures of ILs and PEGs of different molecular weights was originally described by Rogers *et al.*[9] In addition, Rebelo and co-workers[10] demonstrated the existence of salting-in/-out effects of ILs over a high molecular weight PEG in aqueous solutions. According to this sequence, PEG–IL-based ABS were recently proposed by Freire *et al.*[11] who also showed that their phase polarities can be controlled by adequately tuning the chemical structure of the IL. One of the major advantages of these systems relies on the biocompatibility and low toxicity of PEGs. Nevertheless, the systems studied hitherto combine PEGs with ILs that may have non-negligible toxicity, low biocompatibility, and poor biodegradability.[11] Moreover, the large-scale application of these systems may not be achievable due to the high price of the ILs used.[11] The possibility of tuning the IL's structure by independently modifying the structures of both cation and/or anion allows one to design new fluids with an acceptable environmental footprint and enhanced biocompatibility, as well as low cost.

Cholinium chloride (2-hydroxyethyltrimethylammonium chloride, m.p. = 302 °C) is a water soluble essential nutrient important for cell membrane structure and for synthesizing folic acid and vitamin B12.[12] Recent research has demonstrated the synthesis of novel cholinium-based ILs ($[Ch]^+$ ILs) with the cholinium cation being paired with different anions.[13] These ILs present outstanding biodegradability and low toxicity to filamentous fungi and the freshwater crustacean *Daphnia magna*.[14] Furthermore, several articles have described novel $[Ch]^+$ ILs in which protein structure and enzyme function can be maintained or even increased.[15] Due to these and other exceptional properties, interest in these compounds has increased in the past few years, with applications ranging from crosslinking agents for collagen-based materials, to solvents in the pre-treatment and dissolution of biomass, and for use as co-substrates for microorganisms in the degradation of dyes.[16] In addition, this new class of ILs is generally accessible, easy to handle, less toxic and cheaper than the more commonly studied ILs.[16]

Considering the potential application of ABS for the extraction of added-value compounds and their mandatory biocompatibility and biodegradability issues, a new class of ABS composed of $[Ch]^+$ ILs and K_3PO_4 (as the inorganic salt) was recently proposed,[17] while the possibility to form ABS with polypropylene glycol (PPG) and $[Ch]^+$ ILs was also reported.[18] It was suggested that the $[Ch]^+$ ILs can either act as the salting-out species of the moderately hydrophobic PPG or being salted-out by a highly charged density salt.[17,18] In this context, it has been accepted that the molecular level mechanism of the two-phase formation is ruled by the formation of hydration complexes and/or the ions' affinity for water.[17,18] While this seems to be valid for IL–salt-based ABS,[17] the formation of IL–polymer-based systems seems to be by far more complex than usually reported or initially anticipated,[18] and the mechanisms for ABS formation in PPG–$[Ch]^+$ ILs still require further confirmation. For a more hydrophilic polymer, such as PEG, the molecular phenomenon which governs the formation of an immiscible regime is even more intricate.

In order to gather further evidence that could lead to the understanding of the specific interactions dominating the phase behaviour of polymer–IL-based ABS, in this paper, the phase diagrams of several ternary systems composed of water, $[Ch]^+$ salts and PEGs were determined at different temperatures. Several structurally distinct $[Ch]^+$ salts – combined with the anions chloride (Cl^-), bicarbonate ($[Bic]^-$), bitartrate ($[Bit]^-$), acetate ($[Ac]^-$), propanoate ($[Pro]^-$), butanoate ($[But]^-$), dihydrogencitrate ($[DHcit]^-$), glycolate ($[Gly]^-$), lactate ($[Lac]^-$), and dihydrogenphosphate ($[DHph]^-$) – were studied. This series includes salts with high melting temperatures (103–302 °C), two salts with melting temperatures ranging between 38 and 85 °C, and three salts which are liquid at ambient temperature. Three PEGs of different molecular weights (400, 600, and 1000 g mol^{-1}) were also used to evaluate their impact on ABS formation. Moreover, binary PEG–salt and salt–water solubility data, water activities of the various compounds, and binary and ternary excess enthalpies estimated by COSMO-RS (COnductor-like Screening MOdel for Realistic Solvation)[19] were used in a combined strategy to provide novel molecular insights responsible for the observed liquid–liquid demixing behaviour.

Results and discussion

Properties and solubilities of [Ch]-based salts

Cholinium ($[Ch]^+$) salts (commercially acquired or synthesized by us as described in the ESI†) with Cl^-, $[Bic]^-$, $[Bit]^-$, $[Ac]^-$, $[Pro]^-$, $[But]^-$, $[DHcit]^-$, $[Gly]^-$, $[Lac]^-$ and $[DHph]^-$ (Table 1) were used to investigate ABS formation when combined with PEGs. All the salts were characterized for melting points (m.p.) and solubilities in PEG-600 and in water (Table 1). The solubility measurements were carried out at 25 °C and atmospheric pressure, by a gravimetric method described in the ESI.† The salts [Ch][DHcit], [Ch][Bic], [Ch][DHph], [Ch][Bit] and [Ch]Cl present high melting temperatures ranging from 103 to 302 °C. [Ch][Ac] and [Ch][Gly] present a m.p. of 85 °C and 38 °C,[20] respectively, whereas [Ch][But], [Ch][Pro] and [Ch][Lac] are liquid at room temperature.

According to the data presented in Table 1, noteworthy differences in the solubilities of the cholinium-based salts in PEG-600 or in water are observed based on whether the salts are liquid or crystalline species at room temperature (RT). All of the $[Ch]^+$ salts that are liquid at RT are completely soluble in water,

Table 1 Chemical structure of the studied $[Ch]^+$ salts and respective properties

Salts or ILs	Name	Cholinium cation	Anion	m.p./°C	Solubility in PEG 600 / (mol kg^{-1})	Solubility in water/ (mol kg^{-1})	log K_{ow}[a]	Anion polar surface[b]/(A^2)	pK_a of the conjugated acid of the anion[21]
Ionic liquids	Cholinium butanoate ([Ch][But])	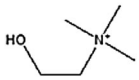	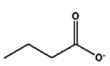	Liquid at RT	Totally soluble	Totally soluble	N.A.[e]	40.13	4.83
	Cholinium propanoate ([Ch][Pro])			Liquid at RT	Totally soluble	Totally soluble	N.A.[e]	40.13	4.87
	Cholinium lactate ([Ch][Lac])			Liquid at RT	Totally soluble	Totally soluble	−3.70	60.36	3.08
	Cholinium acetate ([Ch][Ac])			85	4.473	20.871	−4.66	40.13	4.47
	Cholinium glycolate ([Ch]Gly)			38	3.221	Totally soluble	−1.20	60.36	3.83
Salts	Cholinium dihydrogencitrate ([Ch][DHcit])		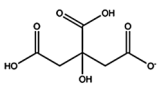	103–107	<0.005	3.295	−1.32 −1.198[c] −1.198[d]	134.96 137.79[c] 140.62[d]	3.13 4.76 6.40
	Cholinium bicarbonate ([Ch][Bic])			114–115	N.A.[e]	24.215	−3.70	60.36	6.37 10.25
	Cholinium dihydrogenphosphate ([Ch][DHph])			119	<0.005	13.450	−3.70	90.40	2.12 7.21 12.67
	Cholinium bitartrate ([Ch][Bit])		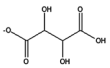	149.5	<0.005	4.824	−1.43	82.06	3.22 4.85
	Cholinium chloride ([Ch]Cl)		Cl^-	302	0.260	21.121	−3.70	—	<1

[a] The log K_{ow} values are a measure of the differential solubility of a particular solute between octanol and water. [b] The anion polar surface value is the surface sum over all polar atoms, primarily oxygen and nitrogen, and also includes their attached hydrogens. [c] Data corresponding to the $Hcit^{2-}$ species. [d] Data corresponding to the cit^{3-} species. [e] N.A.: data not available.

and display the highest solubilities in PEG-600. All of the crystalline salts at RT have a solubility saturation in water, as well as quite limited values of solubility in PEG-600. These differences in water solubility reflect the relationship between the relative solvation energies of the ions *vs.* the crystalline lattice energies of the salts. The completely soluble liquid salts would not have the same competitive formation of a crystalline lattice, even though some contribution from a 'liquid lattice' cannot be ruled out. The differences observed in the solubilities with water and PEG-600 suggest that the interactions and the behaviour in the ABS ternary systems could be directly affected by the physical state of the compounds (liquid or salts) and how they are solvated and interact with each other.

Of all the properties of the salts studied here, the major differences between the higher and lower melting $[Ch]^+$ salts were found for the anion polar surface values, where the higher melting salts have the highest values. In fact, the higher melting cholinium-based salts are those that present a more localized charge, and thus, higher melting temperatures. In addition, all of the higher melting salt anions are from di- or tri-acidic species (with the exception of the quite different Cl^- which has a small localized charge). Therefore, the pH of each system should be kept in mind, since at different pH values the species in equilibrium could change, as then will the respective solvation in aqueous media. A detailed analysis of each species in equilibrium will be carried out (below) in the discussion of the ternary phase diagrams.

In general, the properties and solubilities given in Table 1 suggest distinct breaks between the higher and lower melting salts. Hence, the discussion below of the liquid–liquid demixing behaviour for the aqueous solutions with PEG and $[Ch]^+$ salts will focus on any distinct trends which can be attributed to the different properties between the higher melting salts and the lower melting compounds which tend to fall within the IL categorization.

Phase diagrams: effect of different $[Ch]^+$ salts

PEGs of average molecular weights 400 g mol^{-1} (PEG-400), 600 g mol^{-1} (PEG-600), and 1000 g mol^{-1} (PEG-1000) were used to evaluate the effects of different $[Ch]^+$ salts in aqueous solution, and their ability to form ABS, while confirming a general behaviour independently of the polymer size. Aqueous solutions of each $[Ch]^+$ salt (from 40 wt% to 80 wt%) and of each PEG (from 80 wt% to pure PEG) were initially prepared and used for the determination of the binodal curves at 25 °C (±1 °C) and atmospheric pressure, according to literature procedures.[22]

The room temperature liquid salts [Ch][Pro], [Ch][But], and [Ch][Lac] are totally soluble in both PEG and water. Neither [Ch][Pro] nor [Ch][But] induce biphase-formation with any of

the PEGs and [Ch][Lac] only forms ABS with the higher molecular weights PEG-600 and PEG-1000. All other salts form biphasic systems with all three PEGs.

The composition of each ABS was calculated by the weight quantification of all components added within $\pm 10^{-7}$ kg. The detailed weight fraction experimental data are presented in the ESI† (Tables S1–S12). In most of these systems the bottom phase is the cholinium-rich phase and the top phase corresponds to the PEG-rich phase. However, inversions in the phase densities were observed with [Ch]Cl and [Ch][Ac]. Since both phases are liquid and non-coloured, the coexisting phases were identified by conductivity measurements. In addition, since some of the anions are based on a strong acid, the pH of the co-existing phases was also determined. A detailed description of the properties of each phase, including mixture compositions, pH, and conductivity of the bottom and top phases, is provided in the ESI† (Table S13).

Fig. 1 depicts the solubility curves displayed as initial, total weight fraction of PEG (wt%) *vs.* initial, total molality of salt [mole of salt *per* kg of H_2O]. Molality was chosen in order to avoid distortions in the comparisons that could be a direct consequence of the distinctly different molecular weights of the salts involved. In general, for any mixture composition above the solubility curve there is formation of two aqueous phases whereas below the solubility curve the concentration of each component is not enough to induce the liquid–liquid demixing falling within the monophasic regime.

In all the ABS studied, [Ch][DHph] showed the highest ability to promote ABS, whereas [Ch]Cl exhibited the lowest. In general, the ability of the $[Ch]^+$ salts to promote the formation of ABS with PEG-400, PEG-600 and PEG-1000 follow a quite similar trend, namely: [Ch][DHph] > [Ch][Bit] > [Ch][Bic] > [Ch][DHcit] ≈ [Ch][Ac] ≈ [Ch][Lac] ≈ [Ch][Gly] > [Ch]Cl. It is noteworthy that the two exceptions, the inability of [Ch][Lac] to promote two-phase with PEG-400 (previously highlighted) and the changes exhibited by the [Ch][DHcit] in the binodal shape with different molecular weights of PEGs, suggest more complex speciation which will be discussed in more detail later.

In more conventional systems involving aqueous mixtures of ILs and high charge density salts, the liquid–liquid demixing has been described as a result of a salting-out phenomenon[23] (with the salt ions preferentially hydrated and leading to the exclusion of the more "hydrophobic" IL for a second liquid phase). Previously, Freire and co-workers[17] have shown that $[Ch]^+$ ILs are also capable of forming salt–salt ABS by a salting-out phenomenon induced by a high charge density salt, K_3PO_4. As observed with the majority of IL–salt ABS, this liquid–liquid demixing ability is the result of the high capacity of the high charge density anions to be hydrated.[23] On the other hand, when addressing ABS based on ILs (in which the key is the presence of an organic cation) and hydrophilic polymers, such as PEGs, the magnitude of the ion's hydration capability does not seem to control the major ability to induce phase separation in the respective ABS.[11] In fact, and in contrast to IL–salt-based ABS, where the amount of water is usually higher than 50 wt%,[22,23] in all of the $[Ch]^+$ IL–PEG systems investigated here, the water content is lower than 30 wt% (with the exception of [Ch][DHph]

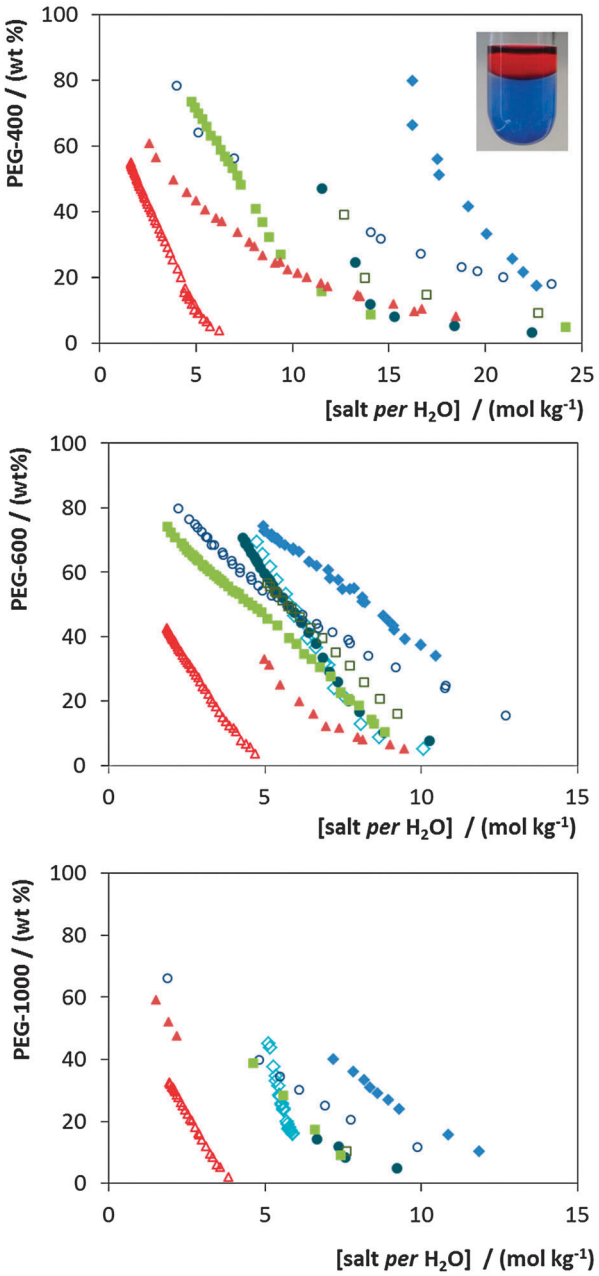

Fig. 1 Experimental solubility data for ABS composed of PEG + $[Ch]^+$ salts at 25 °C: (◊) [Ch][Lac]; (□) [Ch][Gly]; (●) [Ch][Ac]; (○) [Ch][DHcit]; (■) [Ch][Bic]; (△) [Ch][DHph]; (▲) [Ch][Bit]; (♦) [Ch]Cl (axes with different scales). The inset corresponds to the macroscopic appearance of a PEG–cholinium-based two-phase system (the coexisting phases were coloured by the addition of an organic and an inorganic dye).

with *ca.* 50 wt% total water). In most of our examples, there is an approximately 1 : 1 : 1 volumetric fraction of the $[Ch]^+$ salt, PEG, and water. Therefore, the molecular scenario behind the formation of ABS composed of ILs and polymers is consequently more complex.

In contrast to the previous piperidinium-, pyrrolidinium-, and phosphonium-based ionic liquids investigated,[11] the $[Ch]^+$ cation is more hydrophilic, since its three methyl moieties and the hydroxyl group enhance its affinity for water and the

formation of hydration complexes. In addition, PEGs have functional groups with H-bonding donor and acceptor abilities. As a result, the balance of all the binary and specific interactions occurring between $[Ch]^+$/[IL anion]$^-$, $[Ch]^+$/PEG, $[Ch]^+$/H_2O, [IL anion]$^-$/[PEG], [IL anion]$^-$/H_2O, and PEG/H_2O are important to consider.

A review of the data in Fig. 1, particularly those of PEG-600 (Fig. 1b), reveals an interesting phenomenon. Two different shapes are observed for the binodal curves, one for the $[Ch]^+$ salts with relatively high melting points, and another for the $[Ch]^+$ salts with lower melting points or ILs. For the first class of cholinium-based species the binodal curve presents a more intensive dependence on the amount of salt added (at the *xx* axes). We will thus discuss these two classes of salts separately.

Focusing on the PEG-600-based ABS, the abilities of the $[Ch]^+$ ILs ([Ch][Lac], [Ch][Gly] and [Ch][Ac]) to promote an ABS are similar, as are their solubilities with PEG and water (Table 1). Here the balance of interactions between the ions, PEG, and water are fairly close due to the similar H-bonding abilities of the $[Gly]^-$, $[Ac]^-$, and $[Lac]^-$ anions. However, it is important to re-emphasize that [Ch][Lac] is the unique compound that is liquid at room temperature and is able to form ABS. It is noteworthy that this IL does not create an immiscibility region with PEG-400 (neither do the other two liquid salts at RT, [Ch][Pro] and [Ch][But]).

The trend in the ability to induce ABS formation by the higher melting $[Ch]^+$ salts, [Ch][DHph] > [Ch][Bit] > [Ch][Bic] > [Ch][DHcit] > [Ch]Cl, tends to follow the increase in the anion polar surface (which is the surface sum over all polar atoms, primarily oxygen and nitrogen, and their attached hydrogens) and the decrease in lipophilicity reflected by the octanol–water partition coefficients ($\log K_{ow}$) (which are a measure of the differential solubility of a particular solute between octanol and water) – *cf.* Table 1. This fact suggests that the behaviour of the higher melting $[Ch]^+$ salts are governed mainly by solvation in water and their specific affinity for water (where a higher affinity implies a higher ability to promote phase separation). This behaviour is in close agreement with that previously observed in the conventional PEG–crystalline salt ABS, in which the anions with higher charge density are more able to create ion–water complexes and larger repulsive interactions with the ether oxygens of the PEG.[24]

There is, however, an exception with [Ch][DHcit], since this anion should be a stronger salting-out agent, but in our study shows a reduction in the two-phase region, when compared with the binodal curves of the [DHph]-, [Bit]-, and [Bic]-based salts. The $[DHcit]^-$ anion is based on citric acid, which has a high ability to act as a H-bond and/or a H-acceptor. In addition, according to the crystal structure previously studied by Glusker *et al.*,[25] citrate anions can exhibit intramolecular hydrogen bonds between the hydroxyl hydrogen atoms and one of the oxygens of the central carboxyl group. Such self-aggregation would induce a more hydrophobic character to the anion, and decrease its interaction with water and consequently the respective salting-out ability. In this case, the anion–anion interactions may have a larger influence on ABS formation than in the other $[Ch]^+$ salts.

Since the anions are themselves acidic, we investigated the pH of the aqueous solutions of these salts in order to better determine the speciation of ions within these systems (ESI,† Table S13). Based on the dissociation constants of citric acid, $pK_{a1} = 3.13$, $pK_{a2} = 4.76$, and $pK_{a3} = 6.40$,[21] and on the pH of the coexisting phases in the [Ch][DHcit] system (pH = 5 to 6), both the divalent and trivalent anions are in solution. Although a stronger salting-out ability might be expected with a higher valency, there is also a reduction in the anion polar surfaces and higher $\log K_{ow}$ values, for the divalent and trivalent species ($Hcit^{2-}$: $\log K_{ow} = -1.198$ and polar surface area = 137.79 Å^2; cit^{3-}: $\log K_{ow} = -1.198$ and polar surface area = 140.62)[26] which support the reduction in the two-phase region, when compared with the binodal curves of the [DHph]-, [Bit]-, and [Bic]-based salts.

Overall, the phase diagrams suggest different mechanisms for biphase formation for the higher melting $[Ch]^+$ salts *vs.* lower melting $[Ch]^+$ salts or ILs. For the higher melting salts, solvation by water is the main driver for biphase formation as observed in more conventional systems of the type IL + salt, where the ABS formation ability is dominated by the affinity of ILs for water and correlates well with their $\log K_{ow}$ values.[17] This hypothesis is further supported by the strong dependence on the salt *per* water content displayed by the corresponding binodal curves shown in Fig. 1. On the other hand, for the PEG–$[Ch]^+$ ILs systems there is no such correlation with the $\log K_{ow}$ values. The balance of hydrogen-bonding between all the species in equilibrium (cations, anions, PEG, water) are important, as is their respective concentration. ILs with lower affinity for water, *i.e.*, more hydrophobic fluids, are more easily excluded to a second liquid phase. This odd behaviour is thus an indication that the formation of ABS composed of $[Ch]^+$ salts with lower melting temperatures or ILs and PEGs is not merely the consequence of a salting-out effect, but is the result of a more complex balance of the diverse interactions involving all the compounds in equilibrium. Finally, and as depicted in Fig. 1, for the cholinium-based salts there is a less strong dependency on the shape of the binodal curves with the salt *per* water amount.

In order to gather further insights into the dominant interactions occurring in these ABS, the ability of each salt to induce ABS formation was also compared with the solubility of each $[Ch]^+$ compound in PEG-600 (Table 1). As previously discussed, the higher solubility of $[Ch]^+$ ILs in PEG reveals a higher affinity for the polymer and the presence of strong and favourable IL–PEG specific interactions. [Ch][But], [Ch][Prop], and [Ch][Lac], as liquid salts at room temperature, are completely soluble in PEG-600 at all compositions. Thus, it is not surprising that these three $[Ch]^+$ ILs have difficulty in inducing ABS formation. In general, a higher affinity between the PEG and these ILs leads to a lower ability for phase separation in the presence of water.

Phase diagrams: effect of molecular weight of PEG

To gain a further understanding of the effect of the PEG chain lengths on the several systems behaviour, each $[Ch]^+$ salt was plotted in terms of PEG wt% *vs.* [mole of salt *per* kg of H_2O] for the three molecular weights of PEG. The phase diagrams for

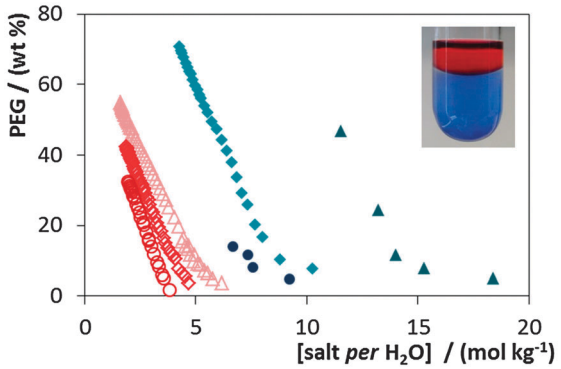

Fig. 2 Experimental solubility data for ABS composed of PEG + $[Ch]^+$ salts at 25 °C: (○) PEG-1000/[Ch][DHph]; (◊) PEG-600/[Ch][DHph]; (△) PEG-400/[Ch][DHph]; (●) PEG-1000/[Ch][Ac]; (♦) PEG-600/[Ch][Ac]; (▲) PEG-400/[Ch][Ac] (axes with different scales). The inset corresponds to the macroscopic appearance of a PEG–cholinium-based two-phase system (the coexisting phases were coloured by the addition of an organic and an inorganic dye).

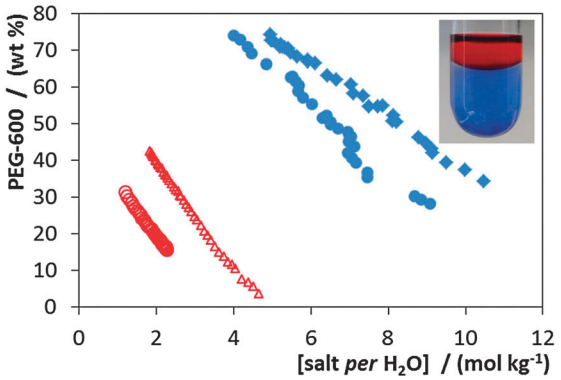

Fig. 3 Experimental solubility data for ABS composed of PEG-600 + $[Ch]^+$ salts: (△) PEG 600 + [Ch][DHph] at 25 °C; (○) PEG 600 + [Ch][DHph] at 50 °C; (♦) PEG 600 + [Ch]Cl at 25 °C; (●) PEG-600 + [Ch]Cl at 50 °C. The inset corresponds to the macroscopic appearance of a PEG–cholinium-based two-phase system (the coexisting phases were coloured by the addition of an organic and an inorganic dye).

[Ch][DHph] and [Ch][Ac] are shown Fig. 2. All other phase diagrams are provided in the ESI† (Fig. S1 to S6).

For all the studied $[Ch]^+$ salts, the ability of the polymer to induce a liquid–liquid demixing follows the order: PEG-1000 > PEG-600 > PEG-400. The same trend is observed in conventional polymer–salt[27] and PEG–imidazolium-based ILs ABS.[11] However, Fig. 2 reveals that for the system composed of [Ch][Ac] and PEG-1000, at concentrations higher than 20 wt% of PEG it is not possible to form ABS. A similar behaviour is observed for [Ch][Gly] (Fig. S5 in the ESI†). This behaviour might be related to both the increasing hydrophobic character of higher molecular weight PEGs, and thus a lower affinity for water, and a decreased miscibility of PEG with the ILs due to a decrease of the hydrogen-bonding donor sites *per* molecule (*i.e.*, the terminal –OH groups on each PEG molecule). The different trends observed with the solid $[Ch]^+$ ILs give the impression that these systems are more complex than observed for the crystalline higher melting salts.

Phase diagrams: effect of temperature

In order to determine the effect of temperature on the ability of liquid–liquid demixing, the ABS of two $[Ch]^+$ salts, [Ch][DHph] (the highest ability to promote phase separation) and [Ch]Cl (the lowest ability to form ABS), were studied at two different temperatures, 25 °C and 50 °C. The respective phase diagrams are presented in Fig. 3, while the detailed weight fraction data are reported in the ESI† (Tables S11 and S12).

The liquid–liquid solubility curves show that, in both systems, an increase in temperature enhances the immiscibility region. This trend is in close agreement with that observed for PEG/salt[28] and PPG/$[Ch]^+$ ABS.[18] In systems covering PEGs and salts, the influence of temperature on the liquid–liquid demixing process seems to be more dominated by the hydrogen-bonding interactions between the PEG and water, and as usually explained, based on the PEG–water lower critical solution temperature (LCST)-type behaviour.[29] For systems dominated by hydrogen-bonding, an increase in temperature leads to a decrease in the interaction strengths and consequently to "easier" liquid–liquid demixing. In this work, an increase in temperature decreases the binary salt–PEG hydrogen-bonding interactions and facilitates the creation of ABS. Therefore, it is clear that in this type of systems hydrogen-bonding plays a dominant role. Partial molar excess enthalpies estimated by COSMO-RS (provided in the ESI,† Fig. S11 and S12) also support this view as discussed below.

Thermodynamic properties of $[Ch]^+$ salts

To additionally evaluate the water–salt and the water–IL interactions (or the ability of the ILs or salts to be hydrated) and their effect upon ABS formation, the water activity of PEG-600 was experimentally determined as a function of the solute molality at 25 °C and compared to those of $[Ch]^+$ salts previously reported by Khan *et al.*[30] (Fig. 4). Water activity corresponds to the ratio between the partial vapour pressure of a solute + water mixture and the standard vapour pressure of pure water, and represents a measure of the intensity with which water associates with a given solute. Since water activity describes the energy status of water in a system, the higher the depression of water activity, the stronger are the interactions between a given solute and water.

The water activity data show that the lower melting $[Ch]^+$ salts or ILs and PEG-600 depress water activity more than the higher melting $[Ch]^+$ salts. Comparing the solubilities of $[Ch]^+$ salts in water and the water activity values, it is observed that the ILs completely soluble in water give lower water activities, as expected. On the other hand, the higher melting $[Ch]^+$ salts exhibit a lower deviation of water activity when compared with pure water.

In summary, there are evident differences between the water activities of the higher *versus* lower melting $[Ch]^+$ salts, which appears to be a correlation between observed water activities and the ability of the IL ions to induce phase separation.

COSMO-RS,[19] a predictive model based on unimolecular quantum chemistry calculations, was finally used to explore the excess enthalpies, H^E, and excess Gibbs free energy, G^E, at 25 °C. The interactions of the binary pairs PEG–water, salt–water, and

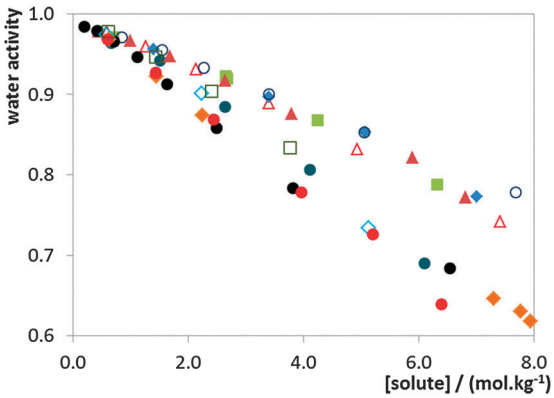

Fig. 4 Experimental water activities at 25 °C: (●) PEG-600; (♦) [Ch][But]; (●) [Ch][Pro]; (◊) [Ch][Lac]; (□) [Ch][Gly]; (●) [Ch][Ac]; (○) [Ch][DHcit]; (■) [Ch][Bic]; (△) [Ch][DHph]; (▲) [Ch][Bit]; (♦) [Ch]Cl. The data shown for the $[Ch]^+$ salts were adapted from Khan *et al.*[30]

salt–PEG and of the ternary mixtures composed of PEG + IL or salt + water, were evaluated, according the procedures described in the ESI.† It should be noted that Khan *et al.*[30] demonstrated the accuracy of COSMO-RS in predicting the water activity coefficients of $[Ch]^+$ salts, and Kurnia and Coutinho[31] confirmed its validity in the prediction of excess enthalpies of water–IL systems. Both previous studies[30,31] support the validity of the COSMO-RS predictions used here to infer upon the main interactions ruling the phase behaviour.

The liquid–liquid equilibrium description by COSMO-RS depicted in Fig. 5 demonstrates favourable interactions between the first two binary mixtures, PEG–water, and IL– or salt–water, as evidenced by the negative H^E and G^E values throughout the whole composition range. Only a measure of the binary for PEG-600 is shown here, as an example. The remaining binary systems with PEG-400 and PEG-1000 are presented in the ESI† (Fig. S7 and S8). In all cases, hydrogen-bonding is the dominant interaction occurring in these binary mixtures. In general, the $[Ch]^+$ ILs display higher energy interactions with water whereas the higher

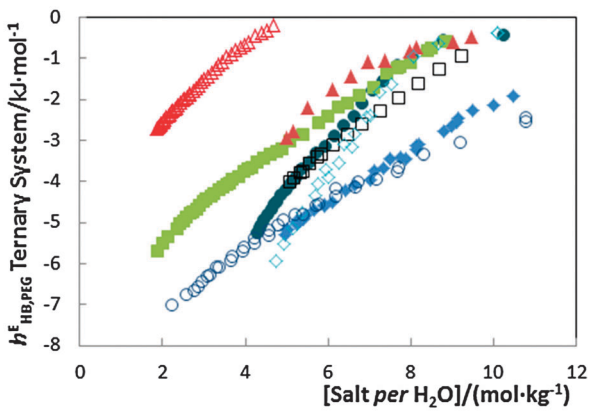

Fig. 5 Partial molar excess enthalpies of the PEG-600 in the ternary system at 25 °C as a function of the concentration of salt per H_2O predicted by COSMO-RS: (△) [Ch][DHph]; (▲) [Ch][Bit]; (○) [Ch][DHcit]; (■) [Ch][Bic]; (◊) [Ch][Lac]; (□) [Ch][Gly]; (●) [Ch][Ac]; (♦) [Ch]Cl.

melting $[Ch]^+$ salts have the lowest values of total energy interactions with water. The unique exception observed for the excess enthalpies is [Ch][Lac]; the energy for this IL is the lowest of all of the ILs investigated.

The estimated partial molar excess enthalpies (h_i^E) of PEG-600 in the ternary system as a function of salt *per* kg H_2O shows that favourable interactions occur between PEG-600 and the anion, in which hydrogen-bonding contributes highly to the exothermicity of the system as shown in Fig. 5. The hydrogen bond strength of PEG-600–$[Ch]^+$ salt can be ranked as follows: $[DHph]^- < [Bit]^- < [Bic]^- < [Lac]^- \approx [Gly]^- \approx [Ac]^- < [DHcit]^- \approx Cl^-$. This sequence closely follows the trend observed in the ability to induce the ABS formation. The Cl^- and $[DHcit]^-$ salts, which have the lowest abilities to promote phase separation, have the strongest interactions with PEG-600 in aqueous media, as reflected by the highly negative h_i^E values. On the other hand, the salts containing the $[DHph]^-$, $[Bit]^-$, and $[Bic]^-$ anions, which have the lowest negative h_i^E values, indicative of weaker interactions, are more capable of inducing liquid–liquid demixing in PEG-based ABS. These results show that ILs with stronger interactions with PEG are less likely to phase separate in aqueous environments and *vice versa*.

It is also interesting to note that the predictive results showed the same trend for the ILs, namely, $[Ch]^+$ salts of $[Gly]^-$, $[Lac]^-$, and $[Ac]^-$. For these compounds, the interactions with PEG-600 are almost the same, supporting the observation of their similar ability to induce the ABS formation. In general, these partial molar excess enthalpies results sustain a competition between the ion–water, ion–ion, and ion–PEG interactions in the ternary mixtures.

In PEG–IL binary systems, a decreased solubility of the IL in the polymer-rich phase with increasing molecular weights was already reported.[9] This pattern was attributed to the lower ratio of terminal –OH groups limiting the sites for hydrogen-bonding with the IL anions.[9] As carried out for the PEG-600 discussed before, COSMO-RS was also used to evaluate the molecular phenomena occurring in the ternary mixtures with PEG-400 and PEG-1000. The respective predicted h_i^E values (shown in the ESI,† Fig. S9 and S10) were also found to be less negative with increased PEG molecular weight, following the same trend observed with PEG-600. In this particular example, electrostatic, hydrogen-bonding, and van der Waals interactions all contribute to less negative values of the enthalpies of mixing.

The salts [Ch][Ac] and [Ch][Gly] are also ILs, albeit crystalline solids at RT. These ILs exhibited the highest solubilities in PEG when compared with all of the higher melting $[Ch]^+$ salts. The binary solubility data here also provide clear evidence that in lower melting $[Ch]^+$ salts or ILs, the PEG–ion interactions are stronger than in the systems with higher melting $[Ch]^+$ salts.

All the results reported in this work support the concept that the ability to promote ABS is different when a salt is crystalline or liquid, as highlighted initially in this paper, because of the corresponding different lattice energies. Nevertheless, it is important to look carefully for some of the exceptions emphasized in this paper, namely with the [Ch][Ac] + PEG-1000, [Ch][Gly] + PEG-1000, and the [Ch][DHcit]-based systems. The first two

exceptions showed the importance of differentiating the ILs that are liquids at RT from the solids. The $[DHcit]^-$ exceptions suggest that this salt cannot be considered simply to be a conventional salt with a m.p. close to 100 °C (103–107 °C) and already falls within the IL categorization.

Conclusions

For the first time it was shown that novel ABS can be formed by the combination of a large array of $[Ch]^+$ salts and PEG polymers at different temperatures. Based on the ternary phase diagrams, solubility data of each $[Ch]^+$ salt in PEG or water, IL or salt water activities, and binary and ternary excess enthalpies, this work demonstrates that for the salts with higher melting points the solvation of the salt anion, and respectively its salting-out ability, seems to be the main driver in the formation of ABS with PEG. On the other hand, it was clearly demonstrated that when salts with lower melting points were used (*i.e.*, the ILs), the ABS formation phenomenon is more complex and directly related to the balance of binary interactions of all the components in equilibrium. Thus, the PEG–IL-based ABS are by far more complex. It is evident that the hydrogen-bonding interactions occurring between the IL anion and the terminal –OH groups of the polymer are more predominant, and further allow the 'tailoring' and more control on the ABS formation ability by increasing the hydrogen-bond donor ability of the respective anion.

In summary, and in contrast to what has been reported, the formation of ABS composed of polymers and ILs is not the main result of a salting-out phenomenon or of the hydration ability of the ions present in the aqueous media. Instead, this liquid–liquid demixing behaviour is a result of a complex hydrogen-bonding competition between all the compounds present in the system – with a clear difference in interactions when these salts have a crystalline or liquid nature.

It was shown that the combination of a large array of $[Ch]^+$ salts and PEGs can form ABS at different temperatures. In addition, most of these ABS are formed by biocompatible and biodegradable salts and polymers. Therefore, the application of these novel systems in separation/purification approaches for the most diverse added-value compounds is the step to follow. Preliminary results for the extraction of tetracycline from a fermentation broth were recently reported by us.[32]

Acknowledgements

This work was financed by national funding from FCT–*Fundação para a Ciência e a Tecnologia* through projects PTDC/QUI-QUI/121520/2010 and Pest-C/CTM/LA0011/2013. The authors also acknowledge FCT for the doctoral grant SFRH/BD/60228/2009 to J.F.B. Pereira and the post-doctoral grant SFRH/BPD/88101/2012 to K. A. Kurnia. M. G. Freire acknowledges the 2012 FCT Investigator Programme.

Notes and references

1 (*a*) P. Å. Albertsson, *Partitioning of Cell Particles and Macromolecules*, Wiley, New York, 3rd edn, 1986; (*b*) J. Huddleston, A. Veide, K. Köhler, J. Flanagan, S.-O. Enfors and A. Lyddiatt, *Trends Biotechnol.*, 1991, **9**, 381–388; (*c*) J. G. L. F. Alves, L. D. A. Chumpitaz, L. H. M. da Silva, T. T. Franco and A. J. A. Meirelles, *J. Chromatogr. B: Biomed. Sci. Appl.*, 2000, **743**, 235–239.

2 (*a*) B. Y. Zaslavsky, *Aqueous Two-Phase Partitioning*, Marcel Dekker, Inc., New York, 1994; (*b*) M. T. Zafarani-Moattar, S. Hamzehzadeh and S. Nasiri, *Biotechnol. Prog.*, 2012, **28**, 146–156; (*c*) Á. S. Lima, R. M. Alegre and A. J. A. Meirelles, *Carbohydr. Polym.*, 2002, **50**, 63–68.

3 (*a*) X. Zeng, J. Quaye and K. Osseo-Asare, *Colloids Surf., A*, 2004, **246**, 135–145; (*b*) F. Spyropoulos, A. Portsch and I. T. Norton, *Food Hydrocolloids*, 2010, **24**, 217–226; (*c*) M. G. Freire, C. L. S. Louros, L. P. N. Rebelo and J. A. P. Coutinho, *Green Chem.*, 2011, **13**, 1536–1545; (*d*) G. B. Cardoso, T. Mourão, F. M. Pereira, M. G. Freire, A. T. Fricks, C. M. F. Soares and Á. S. Lima, *Sep. Purif. Technol.*, 2013, **104**, 106–113.

4 K. E. Gutowski, G. A. Broker, H. D. Willauer, J. G. Huddleston, R. P. Swatloski, J. D. Holbrey and R. D. Rogers, *J. Am. Chem. Soc.*, 2003, **125**, 6632–6633.

5 (*a*) J. S. Wilkes, *Green Chem.*, 2002, **4**, 73–80; (*b*) J. F. Brennecke and E. J. Maginn, *AIChE J.*, 2001, **47**, 2384–2389; (*c*) M. J. Earle and K. R. Seddon, *Pure Appl. Chem.*, 2000, **72**, 1391–1398; (*d*) M. Y. Lui, L. Crowhurst, J. P. Hallett, P. A. Hunt, H. Niedermeyera and T. Welyon, *Chem. Sci.*, 2011, **2**, 1491–1496.

6 M. G. Freire, A. F. M. Cláudio, J. M. M. Araújo, J. A. P. Coutinho, I. M. Marrucho, J. N. Canongia Lopes and L. P. N. Rebelo, *Chem. Soc. Rev.*, 2012, **41**, 4966–4995.

7 (*a*) M. G. Freire, C. M. S. S. Neves, I. M. Marrucho, J. N. Canongia Lopes, L. P. N. Rebelo and J. A. P. Coutinho, *Green Chem.*, 2010, **12**, 1715–1718; (*b*) C. F. C. Marques, T. Mourão, C. M. S. S. Neves, Á. S. Lima, I. Boal-Palheiros, J. A. P. Coutinho and M. G. Freire, *Biotechnol. Prog.*, 2013, **29**, 645–654; (*c*) H. Passos, A. C. A. Sousa, M. Ramiro Pastorinho, A. J. A. Nogueira, L. P. N. Rebelo, J. A. P. Coutinho and M. G. Freire, *Anal. Methods*, 2012, **4**, 2664–2667; (*d*) J. F. B. Pereira, L. P. N. Rebelo, R. D. Rogers, J. A. P. Coutinho and M. G. Freire, *Phys. Chem. Chem. Phys.*, 2013, **15**, 19580–19583; (*e*) J. F. B. Pereira, S. P. M. Ventura, F. A. e Silva, S. Shahriari, M. G. Freire and J. A. P. Coutinho, *Sep. Purif. Technol.*, 2013, **113**, 83–89.

8 J. F. B. Pereira, Á. S. Lima, M. G. Freire and J. A. P. Coutinho, *Green Chem.*, 2010, **12**, 1661–1669.

9 R. D. Rogers, H. Rodriguez, M. Francisco, M. Rahman and N. Sun, *Phys. Chem. Chem. Phys.*, 2009, **11**, 10916–10922.

10 (*a*) J. N. Canongia Lopes and L. P. N. Rebelo, *Chim. Oggi-Chem. Today*, 2007, **25**, 37–39; (*b*) Z. P. Visak, J. N. Canongia Lopes and L. P. N. Rebelo, *Monatsh. Chem.*, 2007, **138**, 1153–1157.

11 M. G. Freire, J. F. B. Pereira, M. Francisco, H. Rodríguez, L. P. N. Rebelo, R. D. Rogers and J. A. P. Coutinho, *Chem.–Eur. J.*, 2012, **18**, 1831–1839.

12 (*a*) A. P. Abbott, G. Capper, D. L. Davies, R. K. Rasheed and V. Tambyrajah, *Chem. Commun.*, 2003, 70–71; (*b*) J. K. Blusztajn, *Science*, 1998, **281**, 794–795.

13 (*a*) J. Pernak, A. Syguda, I. Mirska, A. Pernak, J. Nawrot, A. Pradzynska, S. T. Griffin and R. D. Rogers, *Chem.–Eur. J.*, 2007, **13**, 6817–6827; (*b*) B. Nockemann, B. Thijs, K. Driesen, C. R. Janssen, K. Van Hecke, L. Van Meervelt, S. Kossmann, B. Kirchner and K. Binnemans, *J. Phys. Chem. B*, 2007, **111**, 5254–5263; (*c*) Y. Fukaya, Y. Iizuka, K. Sekikawa and H. Ohno, *Green Chem.*, 2007, **9**, 1155–1157; (*d*) A. J. L. Costa, M. R. C. Soromenho, K. Shimizu, I. M. Marrucho, J. M. S. S. Esperança, J. N. Canongia Lopes and L. P. N. Rebelo, *ChemPhysChem*, 2012, **13**, 1902–1909.

14 (*a*) K. D. Weaver, H. J. Kim, J. Z. Sun, D. R. MacFarlane and G. D. Elliott, *Green Chem.*, 2010, **12**, 507–513; (*b*) M. Petkovic, J. Ferguson, A. Bohn, J. Trindade, I. Martins, M. B. Carvalho, M. C. Leitao, C. Rodrigues, H. Garcia, R. Ferreira, K. R. Seddon, L. P. N. Rebelo and C. Silva Pereira, *Green Chem.*, 2009, **11**, 889–894; (*c*) P. Nockemann, B. Thijs, K. Driesen, C. R. Janssen, K. Van Hecke, L. Van Meervelt, S. Kossmann, B. Kirchner and K. Binnemans, *J. Phys. Chem. B*, 2007, **111**, 5254–5263; (*d*) S. P. M. Ventura, F. A. e Silva, A. M. M. Gonçalves, J. L. Pereira, F. Gonçalves and J. A. P. Coutinho, *Ecotoxicol. Environ. Saf.*, 2014, **102**, 48–54.

15 (*a*) K. Fujita, D. R. MacFarlane and M. Forsyth, *Chem. Commun.*, 2005, 4804–4806; (*b*) K. D. Weaver, H. J. Kim, J. Z. Sun, D. R. MacFarlane and G. D. Elliott, *Green Chem.*, 2010, **12**, 507–513; (*c*) R. Vijayaraghavan, A. Izgorodin, V. Ganesh, M. Surianarayanan and D. R. MacFarlane, *Angew. Chem., Int. Ed.*, 2010, **49**, 1631–1633.

16 (*a*) R. Vijayaraghavan, B. C. Thompson, D. R. MacFarlane, R. Kumar, M. Surianarayanan, S. Aishwarya and P. K. Sehgal, *Chem. Commun.*, 2010, **46**, 294–296; (*b*) Z. Y. Li, X. X. Liu, Y. C. Pei, J. J. Wang and M. Y. He, *Green Chem.*, 2012, **14**, 2941–2950; (*c*) H. Garcia, R. Ferreira, M. Petkovic, J. L. Ferguson, M. C. Leitão, H. Q. N. Gunaratne, K. R. Seddon, L. P. N. Rebelo and C. Silva Pereira, *Green Chem.*, 2010, **12**, 367–369; (*d*) S. Sekar, M. Surianarayanan, V. Ranganathan, D. R. MacFarlane and A. B. Mandal, *Environ. Sci. Technol.*, 2012, **46**, 4902–4908.

17 S. Shahriari, L. C. Tomé, J. M. M. Araújo, L. P. N. Rebelo, J. A. P. Coutinho, I. M. Marrucho and M. G. Freire, *RSC Adv.*, 2013, **3**, 1835–1843.

18 (*a*) Z. Y. Li, X. X. Liu, Y. C. Pei, J. J. Wang and M. Y. He, *Green Chem.*, 2012, **14**, 2941–2950; (*b*) X. Liu, Z. Li, Y. Pei, H. Wang and J. Wang, *J. Chem. Thermodyn.*, 2013, **60**, 1–8.

19 (*a*) A. Klamt and F. Eckert, *Fluid Phase Equilib.*, 2000, **172**, 43–72; (*b*) M. Diedenhofen and A. Klamt, *Fluid Phase Equilib.*, 2010, **294**, 31–38; (*c*) A. Klamt, *COSMO-RS from quantum chemistry to fluid phase thermodynamics and drug design*, Elsevier, Amsterdam, Boston, 2005.

20 Y. Fukaya, Y. Iizuka, K. Sekikawa and H. Ohno, *Green Chem.*, 2007, **9**, 1155–1157.

21 *p*-functions for common acids and bases at http://www.csudh.edu/oliver/chemdata/data-ka.htm, last accessed on 5th February 2014.

22 (*a*) S. P. M. Ventura, C. M. S. S. Neves, M. G. Freire, I. M. Marrucho, J. Oliveira and J. A. P. Coutinho, *J. Phys. Chem. B*, 2009, **113**, 9304–9310; (*b*) H. Passos, A. R. Ferreira, A. F. M. Cláudio, J. A. P. Coutinho and M. G. Freire, *Biochem. Eng. J.*, 2012, **67**, 68–76.

23 (*a*) T. Mourão, A. F. M. Cláudio, I. Boal-Palheiros, M. G. Freire and J. A. P. Coutinho, *J. Chem. Thermodyn.*, 2012, **54**, 398–405; (*b*) C. M. S. S. Neves, M. G. Freire and J. A. P. Coutinho, *RSC Adv.*, 2012, **2**, 10882–10890; (*c*) M. G. Freire, C. M. S. S. Neves, J. N. Canongia Lopes, I. M. Marrucho, J. A. P. Coutinho and L. P. N. Rebelo, *J. Phys. Chem. B*, 2012, **116**, 7660–7668.

24 R. Sadeghi and F. Jahani, *J. Phys. Chem. B*, 2012, **116**, 5234–5241.

25 J. P. Glusker, *Acc. Chem. Res.*, 1980, **13**, 345–352.

26 (*a*) Chemspider, The free chemical database, http://www.chemspider.com;; (*b*) H. Garcia, R. Ferreira, M. Petkovic, J. L. Ferguson, M. C. Leitão, H. Q. N. Gunaratne, K. R. Seddon, L. P. N. Rebelo and C. Silva Pereira, *Green Chem.*, 2010, **12**, 367–369.

27 R. D. Rogers and J. H. Zhang, *J. Chromatogr. B: Biomed. Sci. Appl.*, 1996, **680**, 231–236.

28 (*a*) R. Sadeghi and R. Golabiazar, *J. Chem. Eng. Data*, 2010, **55**, 74–79; (*b*) H. D. Willauer, J. G. Huddleston, M. Li and R. D. Rogers, *J. Chromatogr. B: Biomed. Sci. Appl.*, 2000, **743**, 127–135.

29 V. Fischer, W. Borchard and M. Karas, *J. Phys. Chem.*, 1996, **100**, 15992–15999.

30 I. Khan, K. A. Kurnia, T. E. Sintra, J. A. Saraiva, S. P. Pinho and J. A. P. Coutinho, *Fluid Phase Equilib.*, 2014, **361**, 16–22.

31 K. A. Kurnia and J. A. P. Coutinho, *Ind. Eng. Chem. Res.*, 2013, **52**, 13862–13874.

32 J. F. B. Pereira, F. Vicente, V. C. Santos-Ebinuma, J. M. Araújo, A. Pessoa, M. G. Freire and J. A. P. Coutinho, *Proc. Biochem.*, 2013, **48**, 716–722.